Airborne and spaceborne lidar measurements of water vapor profiles: a sensitivity analysis

Syed Ismail and Edward V. Browell

This paper presents an evaluation of the random and systematic error sources associated with differential absorption lidar (DIAL) measurements of tropospheric water vapor (H_2O) profiles from airborne and spaceborne platforms. The results of this analysis are used in the development and performance evaluation of the Lidar Atmospheric Sensing Experiment (LASE) H_2O DIAL system presently under development at the NASA Langley Research Center for operation on a high altitude ER-2 (advanced U-2) aircraft. The analysis shows that a <10% H_2O profile measurement accuracy is possible for the LASE system with a vertical and horizontal resolution of 200 m and 10 km, respectively, at night and 300 m and 20 km during the day. Global measurements of H_2O profiles from spaceborne DIAL systems can be made to a similar accuracy with a vertical resolution of 500 m and a horizontal resolution of 100 km.

I. Introduction

Water vapor (H_2O) has a strong influence on many atmospheric processes associated with meteorology, climate, and the global hydrologic cycle. Measurements of the spatial and temporal variability of water vapor are important in understanding the hydrologic cycle, global circulation and dynamics, storm phenomena, dynamics of the atmospheric boundary layer, and atmospheric radiative transfer. High vertical resolution (<1 km) measurements over both regional and global scales are needed in these studies. Sparsely distributed radiosonde network stations provide the only sources of global H_2O measurements. Passive remote sensing techniques from space provide global coverage of H_2O distribution but do not provide good vertical resolution.[1] Lidar remote sensing techniques can provide high resolution measurements of H_2O distributions. The Raman lidar technique[2] can provide high resolution (≤100 m) H_2O measurements, but this technique is limited to relatively short (<7 km) vertical ranges. The differential absorption lidar[3,4] (DIAL) method can provide long-range high resolution measurements of H_2O. The DIAL method which has the potential to provide high resolution measurements of H_2O on a global scale if operated from spaceborne platforms, is discussed in this paper.

Although H_2O was first measured in 1966 with the DIAL technique,[5] more extensive H_2O measurements have been made possible from ground-based[6,7,10-12] and airborne[8,9] platforms due to recent DIAL technology developments. As a precursor to the development of a spaceborne DIAL system for global measurement of H_2O profiles, an advanced autonomous DIAL system called the Lidar Atmospheric Sensing Experiment (LASE)[13] is being developed at the NASA Langley Research Center for flight on a high-altitude ER-2, an extended range U-2, aircraft. In recent years several studies[14-18] have also been conducted exploring the potential for DIAL measurements from space.

In this paper we present a comprehensive sensitivity analysis for a nadir-viewing DIAL system for range-resolved measurements of H_2O profiles from an aircraft or space platform. This sensitivity analysis includes potential error sources related to the detection of the lidar signals and to the knowledge of the H_2O absorption cross section. The purpose of this study is to demonstrate the sensitivity of the DIAL H_2O measurement accuracy to atmospheric and instrument parameters and to show that the DIAL systems described have the potential to meet the measurement needs of H_2O in the atmosphere. Any development of a DIAL system should be based on the knowledge of these sensitivities to reduce or eliminate such errors. Because signal errors are dependent on lidar system parameters and range to the measurement region, examples of signal error sensitivities for both airborne and spaceborne platforms are given. For a complete analysis, we use the parameters for the LASE system. Parameters for the lidar atmospheric sounder and altimeter (LASA) DIAL system,[16,17] envisioned for oper-

ation from a polar orbiting satellite are used in the analysis for the measurements of tropospheric H_2O. Even though H_2O absorption lines in the 720-nm band are used in all calculations, the analysis of the DIAL measurement accuracy discussed in this paper is applicable to other bands of H_2O and to other molecules. In the following sections, a general description of the DIAL methodology is presented; the signal detection and absorption cross section errors are evaluated in relation to the LASE and LASA systems; and the combined DIAL measurement errors are discussed.

II. DIAL Method Principles

The simplified DIAL equation[3] for determining the average gas concentration, n, between ranges R_1 and R_2 is given by

$$n = \frac{1}{2\Delta\sigma(R_2 - R_1)} \ln\left[\frac{S_{on}(R_1)S_{off}(R_2)}{S_{on}(R_2)S_{off}(R_1)}\right], \qquad (1)$$

where S_{on} and S_{off} are the lidar signal amplitudes at the on and off wavelengths; the lidar wavelengths are selected to be on the peak of the gas absorption line and in an unabsorbed region off the peak; and $\Delta\sigma$ is the differential absorption cross section between the on and off wavelengths. Eq. (1) assumes that the wavelength separation between the on and off laser lines is small ($\Delta\lambda \leq 0.1$ nm). In this case, aerosol backscatter and atmospheric extinction[19] errors are considered negligible, and the laser lines are selected so that there are negligible interfering gas influences.[20]

On the basis of Eq. (1) DIAL measurement errors can be classified into two categories, signal detection errors and differential absorption cross section related errors. The signal errors treated in the present analysis are random errors due to uncertainties in the detected signals, background signal noise from solar radiation, and errors resulting from detector dark current and amplifier noise. Analyses of signal errors for some representative DIAL systems have been reported in the literature.[3,21,22] Additional errors in the signal detection and processing system for the LASE H_2O DIAL measurements are discussed in the last section of this paper.

Errors due to uncertainties in the knowledge of the differential cross section are caused by atmospheric effects and laser system characteristics. The main atmospheric effects include temperature sensitivities, pressure broadening and pressure shifts of H_2O absorption lines, and Doppler broadening (DB) of the Rayleigh backscattered component of the lidar return. The laser system parameters that influence DIAL measurements include the finite width of the laser line compared to the width of H_2O absorption line, the spectral purity of the laser line, and uncertainty in the knowledge of the laser line position. Because of these systematic influences it is necessary to evaluate the differential absorption cross section, $\Delta\sigma$, as an effective absorption cross section, $\Delta\sigma_{eff}$, which can then be used in the measurement of n using Eq. (1). The concept of an effective cross section and a method for

calculating it from the actual H_2O absorption cross section are discussed in a later section.

An H_2O absorption line is broadened in the atmosphere by two processes, pressure broadening and Doppler broadening, which are represented by the well known Lorentz and Doppler profiles, respectively. In the lower atmosphere (<15 km altitude), pressure broadening is the dominant spectral broadening influence. The pressure broadened linewidth, γ (halfwidth at halfmaximum HWHM), is given by[23-25]

$$\gamma = \gamma_o \frac{P}{P_o}\left(\frac{T_o}{T}\right)^{0.62}, \qquad (2)$$

where P is the atmospheric pressure and T the atmospheric temperature. The line strength S is given by

$$S = S_o\left(\frac{T_o}{T}\right)^{1.5} \exp\left[\frac{E''hc}{k}\left(\frac{1}{T_o} - \frac{1}{T}\right)\right], \qquad (3)$$

where E'' is the energy of the lower state, h is Planck's constant, c is the speed of light, and k is Boltzmann's constant. The Doppler width, γ_D, is given by

$$\gamma_D = \frac{\nu_o}{c}(2kT\ln 2/m)^{1/2}, \qquad (4)$$

where $\nu_o(cm^{-1})$ is the line center position, and m is the mass of the molecule. For DIAL measurements, the H_2O absorption line shape can be represented by the Voigt profile,[26] which in its limits goes to the Lorentz and Doppler profiles. The absorption cross section, $\sigma(\nu)$, using the Voigt profile representation, is given by

$$\sigma(\nu) = \sigma_o \frac{y}{\pi}\int_{-\infty}^{\infty} \frac{\exp(-t^2)}{y^2 + (x - t)^2}dt, \qquad (5)$$

where

$$\sigma_o = \frac{S}{\gamma_D}\left(\frac{\ln 2}{\pi}\right)^{1/2};$$

$$y = \frac{\gamma}{\gamma_D}(\ln 2)^{1/2};$$

$$x = \frac{\nu - \nu_0}{\gamma_D}(\ln 2)^{1/2}.$$

III. DIAL Signal Detection Errors

The lidar signal errors described in this section are the random errors due to uncertainties in the knowledge of the detected signals, errors due to sunlight or moonlight background, and errors due to detector dark current and amplifier noise. For calculating the total signal detection error, the magnitude of the lidar signals, background signal, and detector dark current are computed based upon a set of model atmosphere and DIAL parameters.

Summertime profiles of molecular density, H_2O concentration, atmospheric temperature, and pressure for the mid-latitude region[27] are used in these simulations. The assumed aerosol profile (Fig. 1) is a composite three layer aerosol model containing a 0–2-km boundary layer with a ground visibility of 23 km,[27] a tropospheric model representing clear conditions from 2–10 km, and a background aerosol model above 10 km. ture profile, with a temperature uncertainty of ± 10 K,
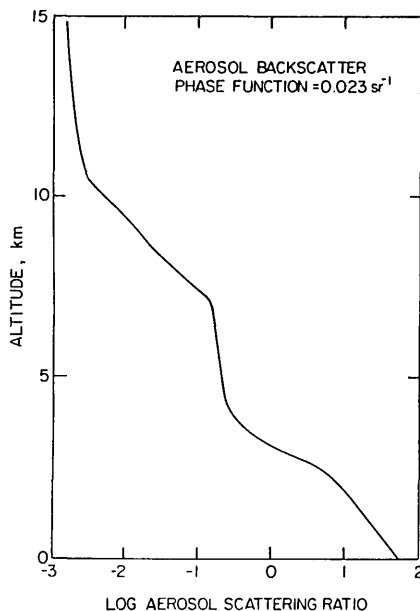
Fig. 1. Assumed three layer aerosol model representing background aerosol conditions with a ground visibility of 23 km. A constant phase function[19] value of 0.023 sr^{-1} is assumed.

The DIAL parameters (Table I) used in these simulations represent parameters of the LASE system.[13] Unless otherwise specified, nominal values of $\lambda = 728$ nm, $\Delta\sigma_o = 20.87 \times 10^{-24}$ cm^2, and $\gamma = 0.1$ cm^{-1} are assumed in these calculations.

The lidar signal S (photoelectrons) from range R is calculated using the expression

$$S(R) = \frac{(E/h\nu)A\eta\beta Qc\Delta t}{2R^2} \exp{-2}\int_o^R \alpha dR \qquad (6)$$

where E [J] is the laser pulse energy, A is the effective area of receiver, η is the quantum efficiency of the

Table I. LASE H₂O DIAL Parameters

| *Transmitter*	
Energy per pulse	150 mJ (on & off)
Rep Rate	5 Hz
Wavelength	726.5–732.0 nm
Beam divergence	0.73 mrad
Pulse width	300 ns
Aircraft altitude	16–21 km
Aircraft velocity	200 m/s
Laser spectral width	1.1 pm
Tuning error	0.25 pm (1σ)
Laser centroid measurement uncertainty	±0.25 pm (1σ)
Laser spectral measurement resolution	<0.5 pm
Spectral purity	>0.99 (0.9995 expected)
Receiver	
Area (effective)	0.11 m^2
Field of view	1.23 mrad
Filter bandwidth (FWHM)	0.4 nm (day); 1 nm (night)
Optical transmittance (total)	29% (day); 49% (night)
Detector efficiency	80% APD (Si)
Noise eq. power	2 × 10^{-14} W Hz$^{-1/2}$
Excess noise factor	2.5
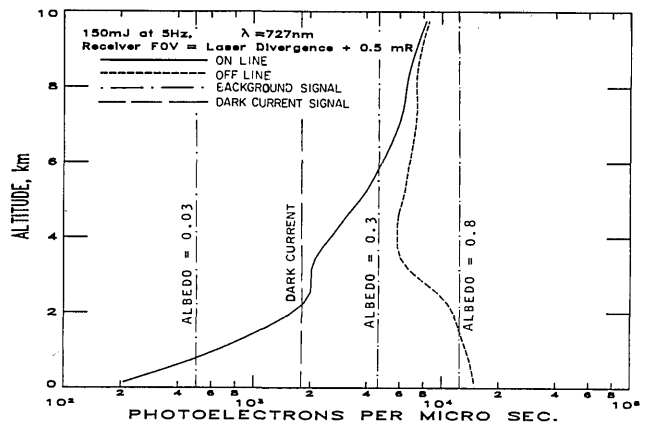
Fig. 2. Lidar signals, detector dark current, and background signal levels for the LASE system operating from an aircraft altitude of 16 km for ground surface reflectivity values of 0.8, 0.3, and 0.03.

detector, β [sr^{-1} km^{-1}] is the total atmospheric volume backscattering coefficient, Q is the total optical efficiency of the receiver for the signal accumulation time Δt, and α is the atmospheric extinction coefficient including the absorption by H$_2$O. The background signal B (photoelectrons), assuming a Lambertian surface and zenith sun, is calculated from the expression.

$$B = \frac{L}{h\nu} \cdot \frac{\rho}{\pi} \cdot \pi\left(\frac{\theta}{2}\right)^2 AwQ\eta\Delta t \exp(-2\tau), \qquad (7)$$

where L is the solar irradiance[28] value (1300 W m^2 μm^{-1}) at 728 nm for a nominal two-way optical depth 2τ of 0.5, w is the optical filter width (FWHM, Table I), ρ is the surface reflectance, and θ is the receiver field of view. The dark current D (photoelectrons) is calculated from the expression

$$D = \left(\frac{\text{NEP}}{\sqrt{2}} \eta \frac{\lambda}{hc}\right)^2 \Delta t, \qquad (8)$$

where NEP is the noise equivalent power.[29] The NEP value used in this study represents the effective noise output of the detector–amplifier system measured in the absence of a lidar signal and day background. The magnitudes of the atmospheric backscattered lidar signals, the day background, and the dark current values calculated using the LASE parameters (Table I) are shown in Fig. 2. The daytime background signals with zenith sun conditions and three surface reflectance values[30] of 0.03, 0.3, and 0.8 for water; vegetation or soil; and snow or low cloud conditions, respectively, are shown in this figure. The nighttime background for the worst case of a full moon condition is a factor of 10^{-5} lower[31] than the values given in Fig. 2.

The detectors used in the LASE system are silicon avalanche photodiodes (Si:APD). The Si:APD has a high quantum efficiency, ~80% at 728 nm, and also high detector noise compared to Photomultiplier Tubes (PMTs). An analysis[32] of the performance of Si:APDs for the LASE system showed that; in this case, because of the strong atmospheric signals, the advantage due to the high quantum efficiency more than offsets the disadvantages due to their higher

noise. In addition, Si:APDs[29] have shown linear detector response over a wide input signal range (10^{-14}– 10^{-8} W) and show excellent impulse response characteristics.

The random error in the measurement of a signal S is calculated from Poisson statistics as $\sqrt{S}$. For an avalanche photodiode (APD) an additional factor called the excess noise factor[29] F must be included to account for the nonuniform gain multiplication in the diode. With this factor, the random error for the same signal is given by $\sqrt{SF}$. Assuming that: (i) the random errors can be combined from all sources [see Eq. (1)] according to the sum of the squares of individual errors and (ii) the s signals are not correlated, the relative error in the DIAL measurement of n is given by

$$\frac{\Delta n}{n} = \frac{1}{2\Delta\sigma n(R_2 - R_1)} \left\{ \sum_{i=1}^{2} \sum_{j=1}^{2} \left[\frac{(S_{ij} + B)F + D}{S_{ij}^2} \right] \right\}^{1/2}, \quad (9)$$

where $i = 1,2$ is for the ranges R_1 and R_2, respectively, and $j = 1,2$ is for the on and off signals, respectively. Equation (9) is a modified form of Eq. (9) of Ref. 22. It can be used to optimize the lidar parameters, to select the optimum detector system, and in random error calculations.

The LASE detector and signal processing system is being developed to achieve two objectives: 1) to cover the expected dynamic range $>10^5$ from the cloud or ground off-line signals to the weak on-line signals from a clean atmosphere and 2) to prevent degradation of the signal-to-noise ratio (SNR) due to the addition of the digitization errors by no more than 10%. To achieve these objectives the signal is divided into a 9:1 ratio and channelled to two Si:APD detectors. The low signal detector is primarily intended to measure the strong ground and cloud returns with a 12-bit digitizer. The primary objective of this is for column H_2O measurements. The high signal (90% energy) detector is intended to measure atmospheric signals. The output of this detector is amplified and digitized by two 12-bit digitizers. The signal from one digitizer A is amplified so that for the weakest atmospheric signals the SNR is not degraded by $>10\%$ by the digitizer random error. The signal amplification for the second digitizer B is set so that digitizer B, at signal levels where A is saturated, does not degrade the SNR by $>10\%$. In our computation of the errors, the random errors are multiplied by a factor of 1.1 to take into account the digitizer error.

The nighttime random error profiles for four H_2O lines with two-way optical depths from 2.2 to 16.2 are shown in Fig. 3. This figure shows that stronger absorption lines are more suitable for DIAL measurements at higher altitudes and that at least two lines are needed to optimally make H_2O measurements over the entire 0–10-km altitude range. Even though the random part of the DIAL measurement error (Eq. 9) depends only on the signals and the local optical depth across the range cell, the minimum error for each of the four profiles in Fig. 3 was at a one-way optical depth of $\sim$1. This result is consistent with the calculations of Remsberg and Gordley (1978).[22] The relationship of
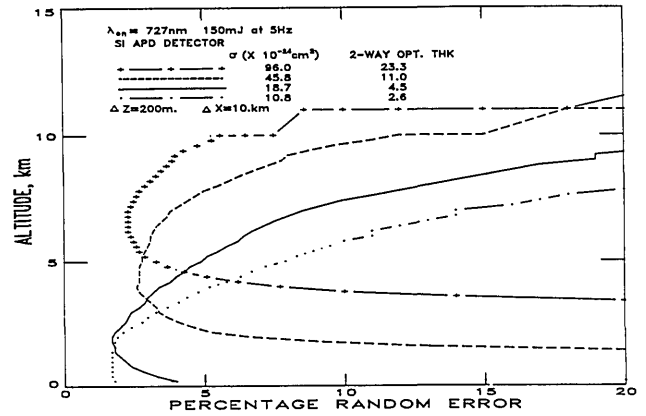

Fig. 3. Random error profiles for the LASE H_2O DIAL system operating with night background conditions. A midlatitude summer H_2O profile[27] is assumed.
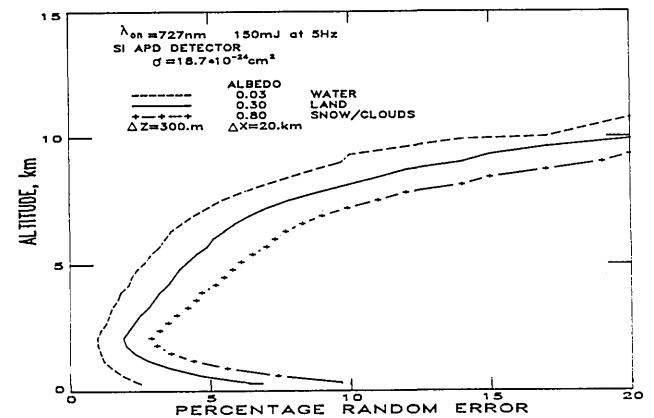

Fig. 4. Random error profiles for the LASE H_2O DIAL system operating over various daytime background conditions.

the random error to the horizontal averaging (achieved by averaging a number of laser shots along horizontal distance x) and vertical smoothing (along R) can also be obtained from Eq. (9). By averaging DIAL measurements from N independent shot pairs, where each shot pair samples the same atmospheric volume and where the gas profile does not change across the N shot pairs, the standard error is expected to decrease as $1/\sqrt{N}$. (This relation holds for near UV DIAL systems[33] and mid-IR DIAL systems[34]). If Δx is the horizontal distance covered during N shot pair measurements, $\Delta n/n \propto \sqrt{1/\Delta x}$. For night background conditions, where $S \gg B$, increasing the range cell size increases the amount of signal received, and therefore from Eq. (9), $\Delta n/n \propto 1/\Delta R^{1.5}$. Therefore, the combined dependence of the measurement error on horizontal averaging and range cell size is given by

$$\frac{\Delta n}{n} \propto (\Delta x)^{-0.5}(\Delta R)^{-1.5}, \quad (10)$$

and for conditions where $S \ll B$ (for example when the day background is unfiltered) $\Delta n/n \propto \Delta x^{-0.5} \Delta R^{-1.0}$.

The signal error profiles for the LASE system during daytime operation are shown in Fig. 4 for the three day
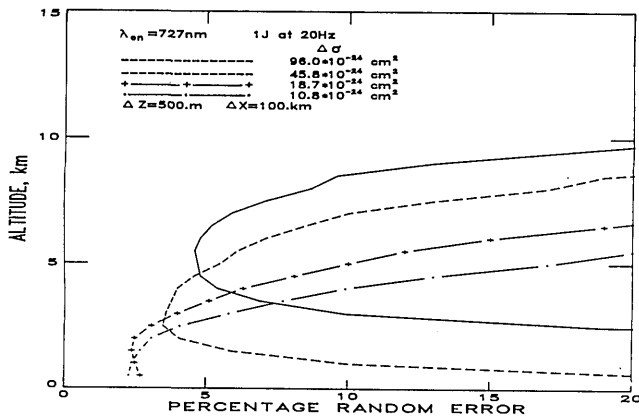
Fig. 5. Random error profiles for a spaceborne H_2O DIAL system at an altitude of 700 km. A summer H_2O model is assumed.

background conditions identified in Fig. 2. To maintain a measurement accuracy for the daytime conditions comparable to those at night, the horizontal averaging (Δx) and the range cell size (ΔR) are increased to compensate for the lower optical throughput of the interference filter and the increased noise due to daytime background. Over water, except for sun glints, there is very little influence of solar background (see Fig. 2), and Eq. (10) is expected to hold over most of the range. Figure 4 shows that with the LASE system, daytime measurements of water vapor profiles are possible even under high background conditions, such as those over the clouds and snow.

Browell et al.[16] have presented simulations which show the feasibility of making DIAL H_2O profile measurements from space. To partially compensate for the $1/R^2$ loss in the lidar signal, both the laser energy and collection area need to be increased over those used in airborne systems. Using a nominal spacecraft altitude of 700 km, a receiver area of 1.1 m², a laser energy of 1 J, and a detector quantum efficiency of 0.2, it is found that the signals from a spaceborne lidar system are smaller by a factor of ~115 compared to the LASE system. This requires a detector system operating in the photon counting mode for measurement of the clear atmospheric returns and in the analog mode for stronger signals from aerosol layers, the ground, and clouds. Figure 5 shows signal error profiles, calculated using the lidar parameters from Table II, for a spaceborne H_2O DIAL system. Larger spatial averaging ($\Delta z = 500$ m; $\Delta x = 100$ km) and higher laser pulse repetition rates (>20 Hz) for spaceborne DIAL systems are necessary to reduce measurement errors to a level adequate for global scale investigations. The main difference between the random error profiles of the LASE system (Fig. 3) and spaceborne system (Fig. 5) occurs at high altitudes (>10 km). For example, at 10 km, the random errors of the LASE and the spaceborne systems are ~5% and >20%, respectively. In the case of the LASE system the decrease in the atmospheric backscattering with altitude is more than compensated by the $1/R^2$ increase in the signal. For the spaceborne system this range dependence is small and

consequently the combination of low atmospheric signals and low differential optical depths results in large random errors. Therefore, for high resolution DIAL H_2O measurements at high altitudes, selection of stronger H_2O absorption lines from the 940-nm and 1140-nm bands[35] is necessary. Browell et al.[16] showed that spaceborne DIAL H_2O profile measurements in the daytime are possible using a narrow receiver field-of-view (0.1 mradian) and a Fabry-Perot interferometer to act as a filter in rejecting background.

In addition to the signal induced uncertainties discussed above, absorption cross section errors also contribute to the total error budget. But unlike the signal errors, which are range dependent, the cross section error is independent of the altitude of platform provided that the platform is above ~20 km because the optical depth above this altitude is <0.01 for the 720-nm H_2O band.

IV. Cross Section Errors

Errors in the DIAL measurement of gas profiles are also caused by uncertainties in the knowledge of the gas absorption cross sections at the remote atmospheric scattering volume. This problem is most severe when narrow absorption lines are used for DIAL measurements, e.g., H_2O. In addition to DIAL system characteristics, atmospheric effects can cause uncertainties in the knowledge of the absorption cross sections. The following systematic effects can produce uncertainties in the absorption cross sections used in the DIAL calculations:

(1) Modification of the laser spectral profile by molecular absorption,

(2) Doppler broadening of the elastically backscattered signal and other atmospheric spectral broadening effects,

(3) Pressure shifts of absorption lines,

(4) Temperature sensitivity of absorption lines,

(5) Laser spectral purity,

(6) Laser wavelength uncertainty, and

(7) Knowledge of laser spectral output.

These effects are caused by atmospheric influences (1)-(4) or DIAL system influences (5)-(7). The spectral widths of the lidar pulses are in general finite compared to H_2O absorption linewidths. With this condition, it is necessary to calculate the effective val-

Table II. Parameters of a Spaceborne Water Vapor DIAL System

Transmitter	
Pulse energy	1 J
Divergence	0.1 mrad
Pulse rep. rate	20 Hz (on and off)
Wavelength	727 nm
Altitude	700 km
Velocity (ground)	7 km/s
Receiver	
Effective area	1.1 m²
Field of view	0.1 mrad
Filter bandwidth (FWHM)	0.01 nm (day); 1.0 nm (night)
Optical transmittance (total)	30% (day); 55% (night)
Detector quantum efficiency	20%
Noise eq. power	2×10^{-15} W Hz$^{-1/2}$

ue of the absorption cross section, σ_{eff} which is a convolution of the lidar spectrum with the absorption line. The value of σ_{eff} is then used in place of $\Delta\sigma$ in calculating n from Eq. (1). Assuming that the off-line absorption is negligible, the effective absorption cross section is given by the equation.

$$\sigma_{eff}(z) = \frac{\int G(\nu,z)\sigma_v(\nu,z)\,d\nu}{\int G(\nu,z)\,d\nu},\quad (11)$$

where $G(\nu,z)$ is an altitude-dependent on-line lidar spectral intensity profile and $\sigma_v(\nu,z)$ is the Voigt absorption cross section profile. Equation (11) is nonlinear, and it can be evaluated numerically for any laser spectral shape. In our evaluation of Eq. (11), we use 200 spectral intervals across the H_2O line profile, and make computations at 1-km altitude intervals. These calculations are for both the forward propagating and backscattered beams because the spectral distribution G is expected to be different for the two cases. To evaluate the error, we simulate a DIAL measurement retrieval. First, the lidar return signals are calculated using a set of lidar parameters and including the effects of atmospheric influences. The effective absorption cross section values are computed using the assumed lidar parameters and estimated atmospheric effects, which are in error compared to the real values used in the signal calculations. Using the simulated signals and the calculated absorption cross sections, we obtain the retrieved DIAL H_2O concentration profile. The error in the DIAL measurement is the difference between the actual H_2O profile used the in signal calculations and the retrieved profile. For the sensitivity analysis, each parameter is independently varied while holding all other parameters constant. However a complete evaluation must include the coupled effects between the various parameters. Therefore following the parametric study an example is discussed which combines all parameters that are likely to influence the DIAL H_2O profile measurements.

(1) Modification of Laser Spectral Profile by Molecular Absorption

As a laser beam is propagated in an absorbing atmosphere, its spectral shape is altered[36,37] due to the absorption. The effective H_2O absorption cross section changes due to this effect and leads to an underestimation in the DIAL determination of H_2O concentrations. The error from this effect is a function of optical depth and laser linewidth. The results of our analysis of this effect are shown in Fig. 6 for a H_2O absorption cross section of 70.1×10^{-24} cm^2. The three profiles show the effect for three laser linewidths (1, 2 and 4 pm), where the laser line consists of three equal-amplitude, equally spaced monochromatic modes across the specified linewidth. Figure 6 shows the influence of optical depth, which increases towards lower altitudes, and larger laser linewidths on the DIAL H_2O density error. Clearly larger linewidths are not suitable for DIAL measurements at large optical
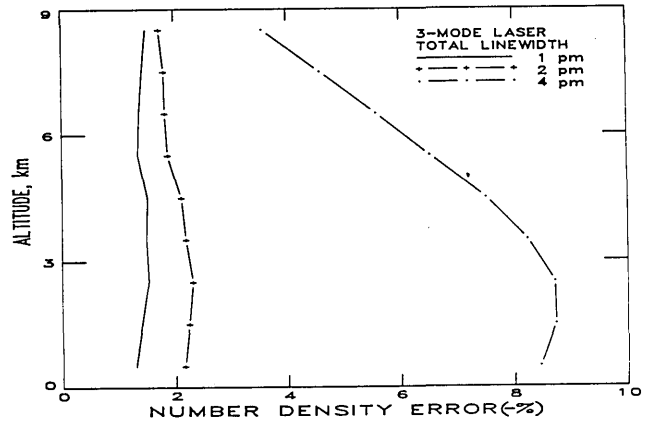

Fig. 6. Influence of laser spectral width causing systematic errors due to the distortion of the laser profile. An H_2O cross section of 70.1×10^{-24} cm^2 is assumed.

depths. Cahen and Megie[36] also evaluated the influence of laser linewidths on DIAL H_2O measurements and showed that if laser linewidths comparable to absorption H_2O linewidths are used, DIAL measurement errors up to 25% can result. In the absence of atmospheric processes that broaden the laser linewidth, the conclusion would be to use the narrowest laser linewidth to minimize the DIAL measurement errors.

(2) Doppler Broadening of the Elastically Backscattered Signal and Other Atmospheric Spectral Broadening Effects

The spectral distribution of laser energy is modified in the backscattering processes due to the motion of atmospheric gases and aerosols. This Doppler broadening (DB) effect on lidar backscatter returns has been extensively discussed in the literature.[37-44] Aerosol particle velocities in the atmosphere are several orders of magnitude lower than those of air molecules and hence the Doppler broadening effect due to aerosols is expected to be negligible ($\ll 0.1$ pm). For simplicity, the velocity distribution of molecules can be assumed to be given by the Maxwellian function. Therefore, the velocity distribution function, $f(v)$, in a given direction is represented by

$$f(v) = \left(\frac{m}{2\pi kT}\right)^{1/2} \exp\left(-\frac{mv^2}{2kT}\right),\quad (12)$$

where m is the average mass of the air molecules. The Doppler shift for the case of the elastically backscattered radiation is given by the equation

$$\frac{\lambda - \lambda_o}{\lambda_o} = -\frac{2v}{c},\quad (13)$$

where λ_o is the incident wavelength, and λ is the Doppler shifted wavelength. The wavelength distribution of the elastically backscattered photons is given for $p < 1$ atm by

$$F(\lambda) = A \exp\left(-\frac{mc^2}{8kT}\right)\left(\frac{\lambda - \lambda_o}{\lambda}\right)^2,\quad (14)$$

where A is a normalizing constant. The DB halfwidth

γ is the distance from line center to the position where the intensity drops to $A/2$. Therefore, from Eq. (14) we get

$$\gamma = \frac{2\lambda}{c} \sqrt{\frac{2kT \ln 2}{m}} . \qquad (15)$$

The value of γ for $\lambda = 727$ nm at 300 K is ~ 1.7 pm, and the altitude variation of the DB full linewidth (2γ) for the given model temperature profile is shown in Fig. 7. This figure also shows the altitude variation of the H_2O absorption linewidth, assuming a Voigt line dependence. From Fig. 7 it is clear that the DB effect has a significant influence on the effective absorption cross section and that this influence is considerable at high altitudes (>5 km) because of the combination of smaller H_2O linewidths and the decrease of aerosol scattering. The altitude variation of the systematic underestimation of the water vapor number densities resulting from no corrections for the DB effect is shown in Fig. 8 (solid line). As expected, the DB has a larger influence at high altitudes, and the error also depends upon the aerosol-to-molecular backscatter ratio at all altitudes. The influence of the three layer aerosol model (Fig. 1) can be seen in Fig. 8. While the influence of DB can be large ($\sim 12\%$ DIAL measurement error at 15-km altitude), it can be corrected to first order with some knowledge of the aerosol-to-molecular backscatter ratio and the temperature profile. Figure 8 (dotted line) shows the residual error due to Doppler broadening effects when the influence of DB is calculated using a 50% error in the estimated aerosol-to-molecular backscatter ratio[45] (with a minimum 20% error in the knowledge of the total scattering ratio) and a 3% (± 10 K) temperature error. These are combined together to produce the worst case undercorrected error. It is assumed that the aerosol-to-molecular backscatter ratio can be derived from the off-line return signal, and a climatological model temperature profile can be used for the temperature profile. These calculations (Fig. 8) show that the residual DB effect, after being partially corrected, causes $\sim 1.5\%$ error below 10 km altitude in the absence of large aerosol gradients.[41] It has been shown by Ismail and Browell[43] that Doppler broadening reduces the sensitivity of DIAL measurement errors to other lidar and atmospheric parameters. This effect is discussed in detail later in this paper.

While Doppler broadening can cause a large systematic error, other spectral broadening mechanisms like Brillouin scattering (BS) and Raman scattering (RS) have smaller influences on DIAL measurements. The BS effect produces two additional peaks in the elastically backscattered signal. Their separation depends upon the velocity of sound, and their intensity depends upon the atmospheric pressure.[46] The BS effect is most pronounced at high pressures (>1 atm). For simplicity it can be modeled as additional broadening of the Doppler profile. For H_2O DIAL systems the BS effect has negligible influence at high altitudes (>10 km) due to low pressures and in the boundary layer due to increased aerosol scattering and a larger H_2O linewidth. The BS effect has its maximum influence
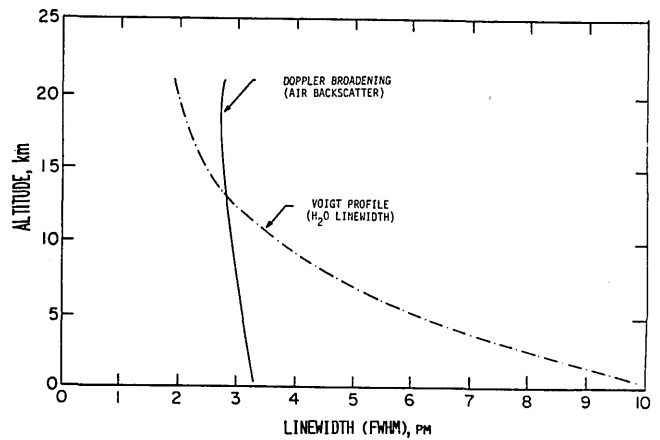

Fig. 7. Comparison of the altitude dependence of the H_2O absorption linewidth and the Doppler-broadened Rayleigh backscattered linewidth.
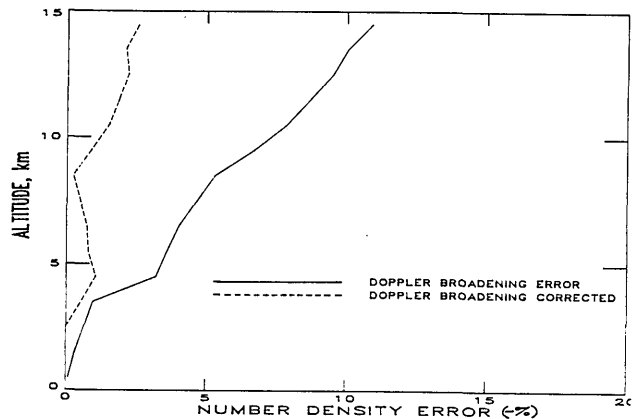

Fig. 8. Systematic error due to Doppler broadening of molecular backscatter in the atmosphere. Also shown is the reduced error profile when Doppler broadening effect is estimated.

in the free troposphere above the boundary layer. An estimate of the magnitude of the BS on the Doppler profile was made from the data obtained by a high spectral resolution lidar system.[40] This measurement indicates that the maximum spectral broadening of the Doppler profile due to BS is <20% at ~ 1 km. We found that in our model calculations the BS increased the DIAL error by <0.5% which is much smaller than the random error or the DB error at this altitude. Thus, the BS error is negligible compared to other error sources in DIAL H_2O concentration measurements.

The Raman scattering (RS) effect generates shifted wavelengths resulting from rotational and vibrational induced transitions. The vibrational Raman spectrum is low intensity (10^{-3} of the unshifted backscattered energy[47]) and is shifted by >50 nm at 727 nm. It can be easily removed by broadband (20 nm) optical filters. The rotational Raman backscatter has an intensity $\sim 3.5\%$ of the elastically backscattered energy[47] from atmospheric molecules. The nearest Raman component is within ~ 0.65 nm of the incident wave-

length, and this effect can influence the DIAL measurements using optical filters with bandwidths larger than 1 nm. The systematic error due to RS increases with optical depth and decreases with increased aerosol backscattering. In a purely molecular atmosphere at large one-way optical depths ($\tau > 2$) with filter widths >20 nm, systematic errors >10% are expected. For H_2O DIAL systems operating at 727 nm it is preferable to filter the rotational RS using an optical filter with <1 nm bandwidth. For such systems the error is negligible (<0.5%) for optical depths up to 4. A general discussion of the influence of the rotational Raman effect on DIAL measurements will be presented in a separate paper.

(3) Pressure Shift

In addition to spectral broadening effects (Eq. 2), changes in atmospheric pressure cause small shifts (~1 pm/atm at 727 nm) in the center position of H_2O absorption lines. Bosenberg[48] has measured shifts for numerous H_2O absorption lines in the 727-nm region, which exhibit an average shift of 0.7 pm/atm. Recently Mandin et al.[49] have published the complete low pressure (nearly vacuum conditions) absorption spectra of H_2O lines in the 725-nm band. Approximate pressure shift values of these lines can be obtained by comparing the line positions determined by Mandin et al.[49] with the ground atmospheric pressure H_2O line positions from the AFGL[35] compilation. A comparison of these line shifts with Bosenberg's measurements show general agreement to within ~20%. If not properly compensated for, these pressure shifts can cause significant errors in DIAL H_2O measurements. The pressure shifts for given altitude, cause the same effect as detuning the laser wavelength off the absorption line center which is discussed later. But unlike the detuning error, the pressure shift error is altitude dependent. If the pressure shift is accurately measured, the DIAL measurement error from it can be fully corrected. Figure 9 shows altitude profiles of the errors caused by a pressure shift of 1.0 pm/atm when the laser line is adjusted to coincide with the peak of H_2O line at ambient pressures equivalent to altitudes of 0, 4, and 20 km. The worst uncorrected error occurs when the laser line is tuned to the peak of the H_2O line at ground pressure and the lidar measurements are made at high altitudes (an error of >16% will result above 14 km altitude). Zuev et al.[50] show that for the 694.38-nm H_2O absorption line (pressure shift 0.91 pm/atm), a DIAL concentration measurement error of 32% will result at 20 km if the laser is tuned to the ground pressure line position. Their results agree with the results shown in Fig. 9. However these calculations are overestimates of the error because the DB influence was ignored. Ismail and Browell[43] show that errors due to pressure shift effects are overestimated by up to 45% when the DB influence is omitted. When the laser line coincides with the peak of the H_2O absorption line at an intermediate altitude of 4 km, the results (Fig. 9) show that very low pressure shift errors (<1%) result over the 0–10 km altitude range of the
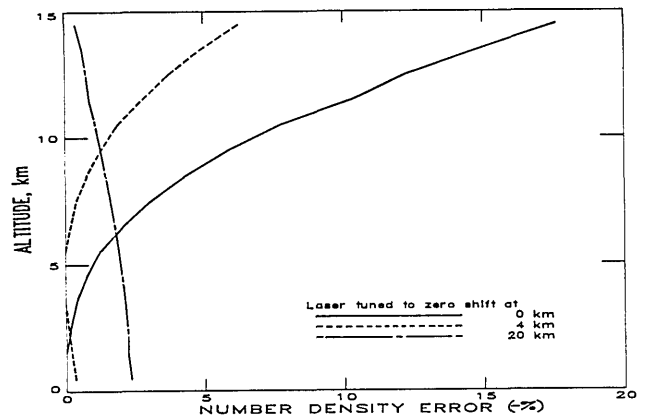

Fig. 9. Systematic errors caused by tuning the laser to H_2O line center at an altitude of 0, 4, and 20 km. A pressure shift of 1.0 pm/atm is assumed.

DIAL measurements. Even these small errors can be removed if the pressure shift is known and accounted for in the DIAL data reduction. Figure 9 also shows that moderate DIAL errors (3%) are caused at ground level when the laser is tuned to the H_2O line peak at an atmospheric pressure representative of 20-km altitude. To minimize the pressure shift error over a broad altitude range, the laser should be tuned towards a lower pressure absorption line center position. This analysis suggests that knowledge of the pressure shift for the H_2O absorption line used in the DIAL measurement is necessary to reduce this systematic error effect to a negligible level (<0.5% from 0–10 km altitude). For the LASE H_2O DIAL system a spectroscopic measurement experiment[54] will measure the pressure shifts to an accuracy of <0.05 pm/atm.

(4) Temperature Sensitivity of H_2O Lines

For DIAL measurements the H_2O lines are selected so that the center line cross section, σ_o, has a small temperature dependence ($\Delta\sigma_o < 1\%$ for a ±10-K change in temperature). Usually the temperature sensitivity of the line center absorption cross section is calculated because most DIAL systems operate with narrow laser lines near the peak of H_2O absorption lines. Previously, temperature sensitivity calculations have been made for H_2O concentration[25] and mixing ratio[7] measurements. Using the Lorentz profile, it can be shown that the condition for temperature insensitive lines for H_2O concentration measurements is given by

$$T_N = \frac{E''hc}{0.88k}, \tag{16}$$

and for mixing ratio calculations by

$$T_N = \frac{E''hc}{1.88k}, \tag{17}$$

where T_N is the temperature at which there is no temperature sensitivity for lines having a ground state energy level of E'' (cm^{-1}). These simplified relationships are approximately valid only near ground atmospheric conditions. For more accurate results a Voigt

model for the H_2O absorption line is necessary. Numerical calculations using the Voigt profile model for DIAL H_2O concentration and mixing ratio measurements and using the most recent H_2O line parameters are reported by Browell *et al.* (1989).[51] These calculations show that for a midlatitude summer atmospheric temperature model and for DIAL measurements near ground the temperature insensitive absorption lines have E'' values in the range 100–250 cm^{-1} for H_2O concentration measurements and E'' in the range 250–450 cm^{-1} for H_2O mixing ratio measurements. These lines cause an error of <1% over a 10 K temperature uncertainty. More details on optimum H_2O line selections in the 720-nm region and their altitude dependence are given in Ref. 51.

(5) Spectral Purity of Lasers

In the DIAL method, the on-line laser energy is assumed to be absorbed by H_2O molecules, and the H_2O concentration is retrieved on the basis of a calculated effective absorption cross section. Many, if not most, laser systems produce small amounts of energy outside desirable spectral limits. The spectral purity is defined, here, as the ratio of the energy within the acceptable spectral limits to the total energy transmitted. In our analysis we assume that the spectral impurity is a component of the laser spectral output that is unabsorbed by H_2O. In some lasers this output results from a broadband emission arising from a process like amplified spontaneous emission (ASE).

Since the spectral impurity is an unabsorbed component of laser energy, the effective absorption cross section is lowered by its presence. The magnitude of the unabsorbed component of laser energy compared to the total energy left in the beam depends on the spectral purity, α, of the transmitted beam and the optical depth for the absorbed portion of the laser output to the range of interest. The unabsorbed energy is treated like off-line energy, and therefore, the on-line signal return from an optical depth (due to H_2O absorption) is given by

$$S_{on} = S_{off}[(1 - \alpha) + \alpha e^{-2\tau}],\qquad(18)$$

where it is assumed that the on- and off-line laser energies are equal initially. For the evaluation of the systematic errors due to spectral purity, the effective cross sections are calculated with and without the spectral purity, and the calculated uncorrected errors that result for spectral purity values of 0.95, 0.99, and 0.9995 are shown in Fig. 10. Small amounts of spectral impurity can produce large systematic errors. For most DIAL applications, lasers with spectral purity >0.99 are necessary if no knowledge of the actual amount of spectral impurity can be obtained. Recently developed Alexandrite lasers, which are being incorporated into various DIAL systems[13,52,53] have been demonstrated to have high spectral purity (0.9999).[53] If the spectral purity of a laser system is known or if it can be calibrated from *in situ* measurements, DIAL measurements are still possible if the spectral purity is lower than 0.99.[9]
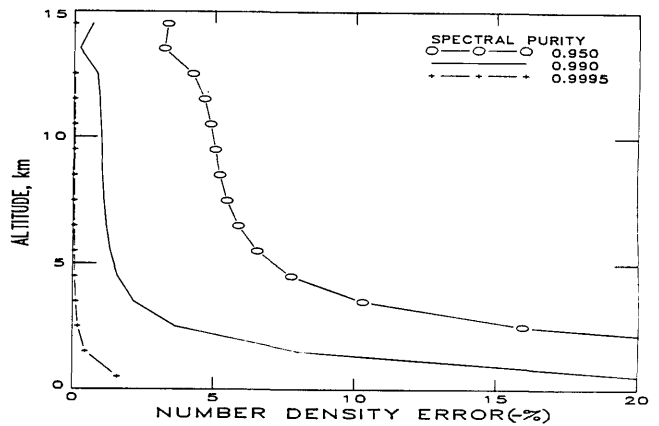

Fig. 10. Influence of spectral purity (caused by ASE) on H_2O DIAL measurements.

(6) Laser Wavelength Uncertainty and Tuning Error

For the operation of most DIAL systems, the on-line laser must be tuned near the center of a gas absorption line. The DIAL measurement error depends upon the uncertainty in the knowledge of the laser position. In addition, the magnitude of this error also depends upon the detuning of the laser from the H_2O line center. Figures 11(a) to 11(c) show the DIAL measurement errors associated with laser line position uncertainty and laser tuning errors with respect to the center of the absorption line. In Figure 11(a) the tuning error is assumed to be zero. Because of the symmetry of the H_2O line, the concentration measurement error depends on the magnitude of the laser line position uncertainty and not on its sign. Figure 11(b) shows that for a tuning error of +0.25 pm the concentration measurement error depends upon both the magnitude as well as the direction of the position measurement error. For a laser detuning of +0.25 pm, because of the symmetry of the H_2O line, a zero concentration measurement error is reached for either a 0 or −0.5 pm position measurement error. On the other hand, for the position measurement errors of +0.25 pm and −0.25 pm, the magnitude and direction of the DIAL errors are different. Figure 11(c) shows that as the tuning error increases to 0.5 pm, the DIAL system becomes more sensitive to position measurement uncertainty. Since the laser line position uncertainty cannot be made zero, a combination of a low tuning error and a low position measurement error is needed to minimize the DIAL measurement error. For the LASE system the tuning error and the position measurement error are both specified to be ≤0.25 pm (1σ).

(7) Wavemeter Resolution

Measurement of the laser spectral profile is needed both in the tuning of the laser system to maintain it within specified spectral position limits and also for calculating the effective cross section in Eq. (11). In the LASE system the laser spectral profile is measured by a wavemeter which samples a small fraction of the laser output. The centroid of the laser spectral profile
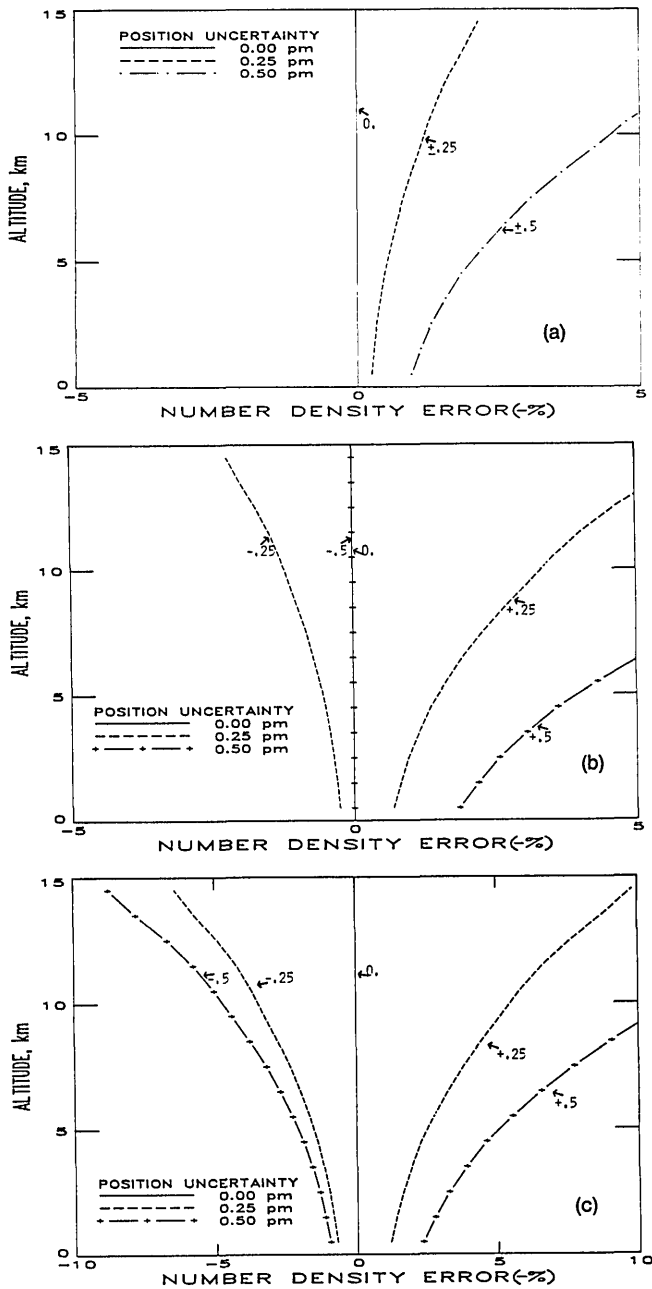
Fig. 12. DIAL systematic error caused by spreading of the laser spectrum by the wavemeter optical resolution.

Fig. 11. H$_2$O DIAL measurement error caused by an uncertainty in the knowledge of laser spectral position (a) no detuning error (b) 0.25 pm detuning error and (c) 0.5 pm detuning error.

measured by the wavemeter is assumed to be the position of the laser. The DIAL error resulting from uncertainties in the laser position measurement have already been discussed in the earlier section. In addition to the position measurement error, the laser spectral profile is broadened due the finite spectral resolution of the wavemeter prior to recording. This spectral broadening makes the calculated effective cross section lower than its actual value, causing the DIAL measurements to be overestimated. Figure 12 shows the results of systematic overestimates in the DIAL concentration measurements for wavemeter resolutions of 0.5 and 1.0 pm. The influence of wave-
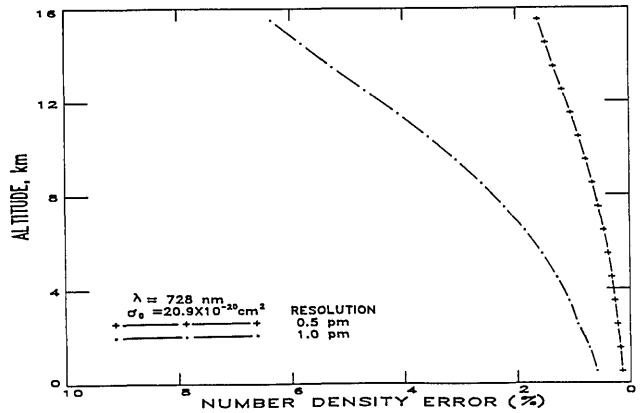
meter resolution increases with altitude because of the decrease in the H$_2$O absorption linewidth. In contrast to other systematic effects like the DB effect, spectral purity, and laser linewidth (which cause an underestimate of DIAL measurements), a wavemeter resolution of 0.5 pm (for the LASE system) causes only a slight overestimate of the density measurement. When other systematic influences are not completely corrected, the residual influence of the wavemeter resolution partially compensates for the other systematic effects. However, if a correction for the other systematic effects is made to achieve a high accuracy (<5% error) H$_2$O measurement, then a wavemeter resolution $\leq$0.5 pm is required, or the wavemeter data must be deconvolved to reconstruct the laser spectral information for each laser pulse.

V. Combined DIAL Measurement Error

The combined DIAL measurement error is the sum of the absolute values of the total random error and the net systematic error. In the signal detection error we include the influence of the detector system, amplifier and digitizer effects, and background signals. In the treatment of systematic effects, we chose to evaluate the influence of each parameter separately; however, in general the selection of any parameter influences the DIAL system's sensitivity to other parameters. In the example of the combined DIAL errors in Fig. 13, the random errors (LASE nighttime case with $\Delta\sigma$ values of 18.7 $\times$ 10^{-24} cm^2 and 90.6 $\times$ 10^{-24} cm^2) are added to the combined systematic error arising from laser line distortion due to H$_2$O absorption, the residual error due to DB, laser detuning of +0.25 pm, laser centroid measurement error of +0.25 pm, and a spectral purity of 0.99. The errors have been combined in such a way that the worst case error is estimated. The wavemeter resolution error is not included because it reduces other systematic errors, and it is assumed that the pressure shift error is fully corrected. The temperature sensitivity error is not included because it is expected to be small. Using the parameters of the H$_2$O absorption lines at 727.8078 nm and at 726.5594 nm in air at STP,[25] and using a climatological tempera-

the DIAL H_2O errors due to temperature effects for the two lines are <0.4% in the 0–5 km altitude region and <0.5% in the 5–10 km region, respectively. To analyze DIAL H_2O data it is necessary to correct for the DB effect. This is because the DB effect can cause large errors (up to 10% below 10 km) even in clean atmospheric regions, and this effect can easily be corrected to first order. For the LASE system spectral purity is expected to be high (>0.9995), and the improvement in the combined error for this spectral purity is represented by the broken line profiles in Fig. 13. This figure shows that by using two H_2O absorption lines with complementary measurement regions in the low and mid-troposphere a total error of <10% over the range 0–10 km can be achieved by the LASE H_2O DIAL system with horizontal and vertical resolutions of 10 km and 200 m, respectively, during nighttime. This result also applies to daytime measurements with horizontal and vertical resolutions of 20 km and 300 m, respectively.

For spaceborne H_2O DIAL measurements in the 720-nm region, the additional optical depth between 20 km and space is expected to be negligible (<0.01). Hence all systematic errors discussed in this paper are also applicable to spaceborne measurements. For space use further refinements in DIAL technology can reduce systematic errors in the DIAL H_2O measurements. In the low altitude region (0–2 km), the random errors of the spaceborne system (Fig. 5) are comparable with the random errors of the LASE system (Fig. 3). Consequently, for low altitude regions, spaceborne measurements of H_2O profiles with a vertical resolution of 500 m and a horizontal resolution of 100 km can be achieved with <10% error during nighttime. Similar measurement accuracies can be made during daytime with resolutions of 500 m and 250 km, respectively. At higher altitudes (2–10 km) further averaging is necessary to achieve a <10% combined error.

VI. Discussion and Conclusions

In the absence of large systematic errors in the DIAL measurement H_2O, the random errors from the lidar signal determine the optimum altitude region for DIAL measurements, and these errors prescribe the amount of horizontal and vertical averaging needed to obtain accurate DIAL measurements. The altitude dependence of the random errors depends upon several factors including detector type, atmospheric background level, atmospheric aerosol distribution, absorption line strength, and the distribution of atmospheric H_2O.

Detector systems with a combination of high quantum efficiency, low excess noise factor, and low noise equivalent power values are desired for H_2O DIAL measurements. Generally for airborne applications, signals are strong (10^3–10^4 photoelectrons/μs) and detectors with high quantum efficiency like Si:APD appear to be optimum[32] in these conditions because their higher quantum efficiency values (0.8–0.9) compared with that of the PMT's (0.04–0.18) more than offset the higher noise of the ADPs. For spaceborne applica-
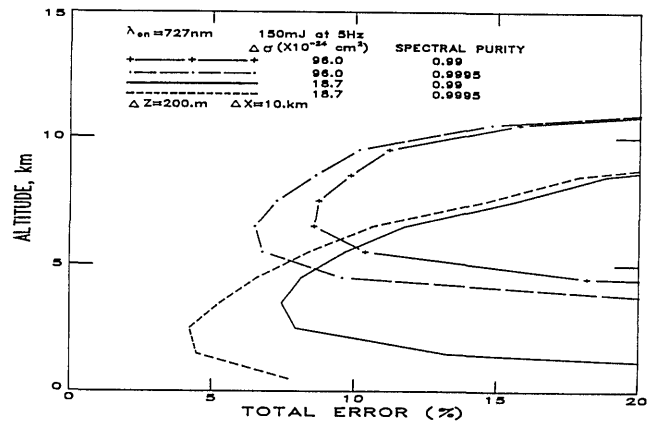

Fig. 13. Combined errors from random and systematic effects in the LASE H_2O DIAL system for two absorption lines. Total DIAL measurement errors are shown for two levels of spectral purity.

tions the signals are expected to be much weaker and low noise detectors with simultaneous analog and photon counting techniques will be necessary. In our analysis of the LASE system we include the total noise from the APD–detector–amplifier system.

We have not considered the influence of signal overload effects in the detector–amplifier system due to clouds. For the LASE system the presence of cirrus clouds can cause significant signal levels 5–60 times[45] the off-line atmospheric signal levels to be expected from low altitudes (<1 km). In addition, atmospheric returns from the near-field can also cause signal overload effects. (Even though the full beam overlap between the transmitter and receiver is expected at a range of >6 km, the signal profile calculation shows that the strongest near-field signal received will be from ~0.5 km range). The LASE system is being designed to be insensitive to the influence of these high signal conditions, and it is expected that the time differences between the near-field region where saturation can occur (10–16 km) and the DIAL measurement region (<10 km) permits sufficient recovery time. However, in the case of the strongest cirrus clouds some degradation of the DIAL measurement is expected. In the case of spaceborne DIAL measurements, no near-field signal effects are expected and the influence of the cirrus clouds has less impact due to the lower signal levels due to the greater ranges involved. Narrow band (FWHM ≤ 0.4 nm) interference filters and receiver field-of-view values of <1 mrad are needed to suppress day background for LASE application and Fabry-Perot interferometer filters along with narrow field-of-view (~0.1 mrad) receivers will be required for daytime DIAL measurements from space.

Generally, H_2O lines with cross section of ~20 × 10^{-24} cm^2 are suitable for DIAL measurement in the low troposphere (<5 km). For an optimum choice of an absorption line, the distribution of H_2O in the region of measurement must be considered as discussed by Browell et al. (1985).[16] Stronger H_2O lines are needed for DIAL measurements at higher altitudes. While H_2O lines in the 720-nm band are adequate for

Remote Sensing: Instrumentation and Techniques, OSA Tech. Digest Series, 18, 22–25 (1987).

13. E. V. Browell, *et al.*, "Development of a High-Altitude H₂O Airborne DIAL System—The Lidar Atmospheric Sensing Experiment (LASE)," *Abstracts, Thirteenth International Laser Radar Conference*, Toronto, Canada, 11–15 Aug. (1986).

14. E. V. Browell and S. Ismail, "Spaceborne Lidar Investigations of the Atmosphere," in *Proceedings, ESA Workshop on Space Laser Applications and Technology*, Les Diablerets, Switzerland, **ESA SP-202**, 181–188, May (1984).

15. M. Endemann, *et al.*, "Orbiting Lidars for Atmospheric Sounding," *Final Report*, Vol. I, Battelle-Institut E. V., Frankfurt, FRG (Dec. 1984).

16. E. V. Browell, S. Ismail, M. P. McCormick, and T. J. Swissler, "Spaceborne Lidar Systems for Measurement of Atmospheric Water Vapor and Aerosols," in *Proceedings, AIAA/NASA EOS Conference*, Virginia Beach, VA, Paper No. 85-2091, Oct. 8–10 (1985).

17. "NASA, Lidar Atmospheric Sounder and Altimeter," *EOS Report*, Vol. 2 (1987).

18. M. J. Kavaya, S. W. Henderson, E. C. Russell, R. M. Huffaker, and R. G. Frehlich, "Monte Carlo Computer Simulations of Ground-based and Space-based Coherent DIAL Water Vapor Profiling," Appl. Opt. **28**, 840–851 (1989).

19. E. V. Browell, S. Ismail, and S. T. Shipley, "Ultraviolet DIAL Measurements of O₃ Profiles in Regions of Spatially Inhomogeneous Aerosols," Appl. Opt. **24**, 2827–2836 (1985).

20. E. V. Browell and P. Woods, *First Int. DIAL Workshop Report*, Virginia Beach, VA, Nov. 1985, NASA Ref. Pub. (1989).

21. R. T. Thompson, Jr., "Differential Absorption and Scattering Sensitivity Predictions," NASA Contract. Rep. 2627 (1976).

22. E. E. Remsberg and L. L. Gordley, "Analysis of Differential Absorption Lidar from the Space Shuttle," Appl. Opt. **17**, 624–630 (1978).

23. R. A. McClatchey, *et al.*, "AFCRL Atmospheric Absorption Line Parameters Compilation," Air Force Cambridge Research Laboratory, Rep. No. TR-0096 Jan. (1973).

24. W. S. Benedict and L. D. Kaplan, "Calculation of Line Widths in H₂O–N₂ Collisions," J. Chem. Phys. **30**, 388–398 (1959).

25. T. D. Wilkerson, G. Schwemmer, B. Gentry, and L. P. Giver, "Intensities and N₂ Collision-Broadening Coefficients Measured for Selected H₂O Absorption Lines Between 714 and 732 nm," J. Quant. Spectrosc. Radiat. Transfer **22**, 315–331 (1979).

26. S. R. Drayson, "Rapid Computation of the Voigt Profile," J. Quant. Spectrosc. Radiat. Transfer **16**, 611–614 (1976).

27. McClatchey *et al.*, "Optical Properties of the Atmosphere," Air Force Geophys. Lab., Hanscom AFB, AFCRL-72-0497 (1972).

28. M. P. Thekaekara, "Extraterrestrial Solar Spectrum, 3000–6100A at 1-A Intervals," Appl. Opt. **13**, 518–522 (1974).

29. P. P. Webb, R. J. McIntyer, and J. Conradi, "Properties of Avalanche Photodiodes," RCA Review **35**, 234–278 (1974).

30. D. E. Bowker, R. E. Davis, D. L. Myrick, K. Stacy, and W. T. Jones, "Spectral Reflectances of Natural Targets for use in Remote Sensing Studies," NASA Ref. Pub., 1139, June (1985).

31. M. L. Wright, E. K. Proctor, L. S. Gasiorek, and E. M. Liston, "A Preliminary Study of Air-Pollution Measurement by Active Remote-Sensing Techniques," NASA-CR-132724, June (1975).

32. R. L. Kenimer, "Predictions of Silicon Avalanche Photodiode Performance in Water Vapor Differential Absorption Lidar," Proc. Soc. Photo. Opt. Instrum. Eng. **889**, 126–135 (1988).

33. M. J. T. Milton and P. T. Woods, "Pulse Averaging Methods for a Laser Remote Monitoring System Using Atmospheric Backscatter," Appl. Opt. **26**, 2598–2603 (1987).

34. W. B. Grant, A. M. Brothers, and J. R. Bogan, "Differential Absorption Lidar Signal Averaging," Appl. Opt. **27**, 1934–1938 (1988).

35. L. S. Rothman, et al., "The HITRAN Database: 1986 Edition," Appl. Opt. **26**, 4058–4097 (1987).

36. C. Cahen and G. Megie, "A Spectral Limitation of the Range Resolved Differential Absorption Lidar Technique," J. Quant. Spectrosc. Radiat. Transfer **25**, 151–157 (1981).

37. C. L. Korb and C. Y. Weng, "The Theory and Correction of Finite Laser Bandwidth Effects in DIAL Experiments," *Abstracts, Eleventh International Laser Radar Conference*, Madison, WI, (1982).

38. G. Fiocco and J. B. Dewolf, "Frequency Spectrum of Laser Echoes from Atmospheric Constituents and Determination of the Aerosol Content of Air," J. Atmos. Sci. **25**, 488–496 (1968).

39. G. Fiocco, G. Benedetti-Michelangeli, K. Maischberger, and E. Madonna, "Measurement of Temperature and Aerosol to Molecule Ratio in the Troposphere by Optical Radar," Nature (London), Phys. Sci., Lett. **229**, 78–79 (1971).

40. S. T. Shipley *et al.*, "High Spectral Resolution Lidar to Measure Optical Scattering Properties of Atmospheric Aerosols. 1: Theory and Instrumentation," Appl. Opt. **22**, 3716–3724 (1983).

41. S. Ismail, E. V. Browell, G. Megie, P. Flamant, and G. Grew, "Sensitivities in DIAL Measurements from Airborne and Spaceborne Platforms," *Abstracts, Twelfth International Laser Radar Conference*, Aix-en-Provence, France (1984).

42. A. Ansmann, "Errors in Ground Based Water-Vapor DIAL Measurements Due to Doppler-Broadened Rayleigh Backscattering," Appl. Opt. **24**, 3476–3480 (1985).

43. S. Ismail and E. V. Browell, "Influence of Rayleigh-Doppler Broadening on the Selection of H₂O DIAL System Parameters," *Abstracts, Thirteenth International Laser Radar Conference*, Toronto, Canada, Aug. 11–15 (1986).

44. A. Ansmann and J. Bosenberg, "Correction Scheme for Spectral Broadening by Rayleigh Scattering in Differential Absorption Lidar Measurements of Water Vapor in the Troposphere," Appl. Opt. **26**, 3026–3032 (1987).

45. P. B. Russell, B. M. Morley, J. M. Livingston, G. W. Grams, and M. Patterson, "Improved Simulation of Aerosol, Cloud, and Density Measurements by Shuttle Lidar," NASA Contractor Report 3473, Nov. (1981).

46. A. H. Lao, P. E. Schoen, and B. Chu, "Rayleigh–Brilliouin Scattering of Gases with Internal Relaxation," J. Chem. Phys. **64**, 3547–3555 (1976).

47. H. Inaba, "Detection of Atoms and Molecules by Raman Scattering and Resonance Fluorescence," in *Laser Monitoring of the Atmosphere*, E. D. Hinkley, Ed. (Springer, New York, 1976), pp. 153–236.

48. J. Bosenberg, "Measurements of the Pressure Shift of Water Vapor Absorption Lines by Simultaneous Photoacoustic Spectroscopy," Appl. Opt. **24**, 3531–3534 (1985).

49. J.-Y. Mandin, J.-P. Chevillard, C. Camy-Peyret and J.-M. Flaud, "The High Resolution Spectrum of Water Vapor Between 13200 and 16500 cm⁻¹," J. Mol. Spectrosc. **116**, 167–190 (1986).

50. V. V. Zuev, Yu. N. Ponomarev, A. M. Solodov, B. A. Tikhomirov, and O. A. Romanovsky, "Influence of the Shift H₂O Absorption Lines with Air Pressure on the Accuracy of the Atmospheric Humidity Profiles Measured by the Differential-Absorption Method," Opt. Lett. **10**, 318–320 (1985).

51. E. V. Browell, S. Ismail, and B. Grossmann, "Temperature Sensitivity of Absorption Lines for H₂O DIAL Measurements," Manuscript in Preparation (1989).

52. C. Cahen, J. L. Lesne, J. Benard, and P. Ponsardin, "A Meteorological (Humidity, Temperature, Aerosols) Mobile DIAL System: Concepts and Design," *Abstracts, Thirteenth International Radar Conference*, Toronto, Canada, 11–15 Aug. (1986).

53. G. K. Schwemmer *et al.*, "A Lidar System for Measuring Atmospheric Pressure and Temperature Profiles," Rev. Sci. Instrum. **58**, 2226–2237, (1987).

54. B. Grossmann and E. V. Browell, *Abstracts, Fourteenth International Laser Radar Conference*, San Candido, Italy, 20–25 June (1988).

DIAL measurements in the 0–10 km altitude region for airborne systems, stronger lines like those in the 940-nm and 1140-nm bands[35] are needed for high resolution spaceborne measurements at >10 km altitude.

Systematic errors in DIAL measurements arise due to uncertainties in the knowledge of the differential absorption cross section between the DIAL wavelengths. These uncertainties are caused by either instrumental or atmospheric effects. The instrumental effects related to the laser spectral width, spectral purity, tuning error, and uncertainties in the knowledge of spectral profiles are discussed in this paper. These parameters can be controlled during the development of a DIAL system. DIAL measurement errors resulting from the modification of the laser spectral profile due to absorption from H_2O in the atmosphere can be evaluated and corrected if necessary during data analysis. Pressure shift errors can be minimized by tuning the laser to coincide with the H_2O line position at the desired altitude or a slightly higher altitude (lower pressure). Temperature sensitivity of H_2O lines can be minimized by selecting the suitable temperature insensitive H_2O lines. The secondary errors introduced by the residual pressure shift and temperature effects can be corrected during data analysis provided that the pressure shift characteristics of the line are known and an estimate of temperature profile can be made.

Doppler broadening plays a significant role in influencing DIAL H_2O measurements, and this effect must be accounted for in the data analysis. In the clean atmosphere it can be removed to first order and in extreme cases of a turbid aerosol layer, it can be ignored. In regions of large vertical inhomogeneity in the aerosol structure the ability to correct the DB effect depends upon the knowledge of the amount of aerosol scattering that can be derived from either the off-line signal[44] or by an independent measurement of aerosol scattering (which may not be practical in all cases). Another aspect of the DB effect which becomes significant[43] at high altitudes (>10 km), is that it reduces the DIAL measurement sensitivity to pressure shifts, changes in the spectral profile in the atmosphere, and laser detuning effects. Another spectral broadening mechanism that can affect DIAL measurements is the rotational Raman scattering by air molecules. The influence of this effect on DIAL measurements of H_2O in the 720-nm region can be made negligible by selecting narrow band (FWHM $\leq$ 3 nm) optical filters.

This analysis of random and systematic influences in DIAL H_2O measurements has been used in the development of the LASE system operating in the 728-nm region and in the analysis of spaceborne DIAL H_2O measurements. The results of this study can be used in testing of DIAL systems, field selection of DIAL parameters, planning data analysis procedures, and in the interpretation and validation of DIAL H_2O measurements. The method discussed in this paper can be easily extended to DIAL H_2O measurements in the 940-nm region, suitable for H_2O measurement at high-

er altitudes (>10 km). The approach is also applicable to the DIAL measurement of other atmospheric gases. We show that a <10% H_2O profile measurement accuracy is possible for LASE with a vertical and horizontal spatial resolution of 200 m and 10 km, respectively, during nighttime and 300 m and 20 km, respectively, during daytime. Global measurements of H_2O profiles from spaceborne DIAL systems can be achieved with similar accuracy with spatial resolutions of 500 m in the vertical and 100 km in the horizontal. We show that the H_2O DIAL systems considered in this analysis can meet the measurement needs for H_2O in the troposphere on regional and global scales.

References

1. C. Prabhakara and G. Dalu, "Passive Remote Sensing of the Water Vapor in the Troposphere and its Meteorological Significance," in *Atmospheric Water Vapor*, A. Deepak, T. D. Wilkerson, and L. H. Ruhrke, Eds. (Academic, New York, 1980).

2. S. H. Melfi, D. Whiteman, R. Ferrare, and V. Falcone, "Observation of Frontal Passages Using a Raman Lidar," *Abstracts, Fourteenth International Laser Radar Conference*, San Candido, Italy, 24–26 June (1988).

3. R. M. Schotland, "Errors in the Lidar Measurement of Atmospheric Gases by Differential Absorption," J. Appl. Meteorol. **13**, 71–77 (1974).

4. R. T. H. Collis and P. B. Russell, in *Laser Monitoring of the Atmosphere*, E. D. Hinkley, Ed., (Springer, New York, 1976), p. 117–151.

5. R. M. Schotland, "Some Observations of the Vertical Profile of Water Vapor by Means of a Ground Based Optical Radar," in *Proceedings, Fourth Symposium on Remote Sensing of Environment*, 12–24 Apr. 1966 (U. Michigan, Ann Arbor, 1966).

6. E. V. Browell, T. D. Wilkerson, and T. J. McIlrath, "Water Vapor Differential Absorption Lidar Development and Evaluation," Appl. Opt. **18**, 3474–3483 (1979).

7. C. Cahen, G. Megie, and P. Flamant, "Lidar Monitoring of Water Vapor Cycle in the Troposphere," J. Appl. Meteorol. **21**, 1506–1515 (1982).

8. E. V. Browell, "Remote Sensing of Tropospheric Gases and Aerosols with an Airborne DIAL System," in *Optical and Laser Remote Sensing*, D. K. Killinger and A. Mooradian, Eds., (Springer-Verlag, New York, 1983), pp. 138–147.

9. E. V. Browell, A. K. Goroch, T. D. Wilkerson, S. Ismail, and R. Markson, "Airborne DIAL Water Vapor and Aerosol Measurements Over the Gulf Stream," *Abstract, Twelfth International Laser Radar Conference*, Aix-en-Provence, France, 13–17 Aug. (1984).

10. V. E. Zuev, Yu S. Makushkin, V. N. Marichev, A. A. Mitsel, and V. V. Zuev, "Lidar Differential Absorption and Scattering Technique," Appl. Opt. **22**, 3733–3741 (1983).

11. W. B. Grant, J. S. Margolis, A. M. Brothers, and D. M. Tratt, "CO_2 DIAL Measurements of Water Vapor," Appl. Opt. **26**, 3033–3042 (1987).

12. J. Bosenberg, "A DIAL System for High Resolution Water Vapor Measurements in the Troposphere," in Laser and Optical